NUMERICAL PREDICTION OF WALL SHEAR RATE IN IMPINGING CROSS-SHAPED JET AT MODERATE REYNOLDS NUMBER

Florin BODE[1,2], Kodjovi SODJAVI[3], Amina MESLEM[3], Ilinca NASTASE[2]

A Computational Fluid Dynamics investigation of impinging lobed jet issuing from a cruciform orifice nozzle was conducted at moderate Reynolds number of 5290, based on the equivalent diameter of the nozzle (De=7.64 mm) and the streamwise bulk velocity (U_0=0.72 m/s). The wall shear rate obtained from numerical simulation is compared to the one acquired experimentally using electro-diffusion technique [1]. The best results were obtained by k-ω based turbulence models. The model with the best accuracy for the present work was k-ω SST, which was the only model that has managed to capture the inflection point on the radial distribution of wall shear rate.

Keywords: impinging jet, numerical simulation, wall shear rate

1. Introduction

Impinging jets have received considerable attention given their many applications connected to the enhancement of mass or heat transfer including industrial processes (paper drying, cooling of heated components of turbine engines and of combustion chambers, cooling of electronic equipments, processing of some metals and glass, deicing of aircraft systems, drying of textile, food products, films and papers, etc [2, 3]). Another type of application is the microenvironment control in personalized ventilation in buildings or vehicles [4]. While for the former, the jet exit Reynolds number falls in general in high or moderate values (> 5000), for the latter, the Reynolds number is low or moderate (from few hundred up to few thousands).

The main objective of this study was to assess the global capability of different turbulence models to capture the flow behaviour in the case of a lobed cross shaped orifice impinging jet. The article presents results issued from a series of experimental and numerical investigations on circular and lobed impinging jets at low and moderate Reynolds numbers including our previous papers [1, 5].

[1] Technical University of Cluj-Napoca , florin.bode@termo.utcluj.ro
[2] Technical University of Civil Engineering in Bucharest, Research Center CAMBI, ilinca.nastase@cambi.ro - corresponding author
[3] University of La Rochelle, LaSIE Laboratory, ameslem@univ-lr.fr

2. Experimental set-up

A schematic diagram of the apparatus used during the experimental part is shown in Fig. 1 b. A small pump is supplied from a reservoir and delivers the fluid to the studied cross shaped orifice. The fluid impinges on the circular target disc provided with six electrodes for electro-diffusion measurements. A detailed description of the theoretical background and electro-diffusion measurement technique can be found in [5].

The temperature of the fluid is controlled within ± 0.2°C. The orifice is mounted on a convergent nozzle and on a 200 mm length stainless steel tube with the inner and outer diameters of 15 and 20 mm, respectively. The tube has been located on a support allowing vertical movement for accurate alignment of the nozzle axis with the electrodes' centre. The reservoir was placed on a sliding compound table allowing movement in the axial and transverse directions of the tube with a precision of 0.05 mm.

The cross orifice has an equivalent diameter of D_e=7.8mm. The orientation of the cross shape with respect to the electrodes was either parallel (0°), i.e. its Major Plane (MP) coincided with electrodes row axis, or the cross was turned with 45° (see Fig. 1 c). In this case, the minor Plane (mP) of the cross orifice nozzle coincided with electrodes row axis.

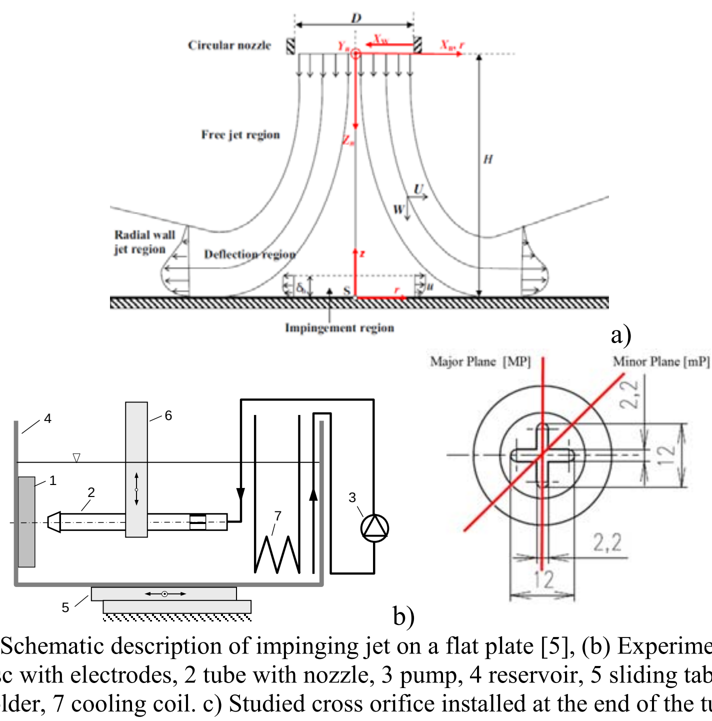

Fig. 1 (a) Schematic description of impinging jet on a flat plate [5], (b) Experimental setup: 1 target disc with electrodes, 2 tube with nozzle, 3 pump, 4 reservoir, 5 sliding table, 6 nozzle holder, 7 cooling coil. c) Studied cross orifice installed at the end of the tube 2

Particle Image Velocimetry (PIV) was employed to acquire instantaneous spatial distribution of the in-plane velocity in the streamwise planes (MP and mP) of the jet flows. A 2D PIV system from Dantec was composed of a FlowSense EO (CCD) camera of 2048×2048 pixels resolution with pixel size of $7.4\times7.4\mu m^2$ and a Quantel BigSky 200 mJ laser. The total field of view is about $2D_e\times3.5D_e$ with a spatial resolution of 27μm per pixel. The acquisition frequency of the PIV system was 15Hz.

Due to the laser reflections at the wall surface, velocity measurements with PIV method very near the targeted are not possible and electro-diffusion method is the most reliable method for measuring the local shear rate/stress in the vicinity of the wall [6].

A detailed description of the experimental systems is given in [1] and [5].

3. Numerical simulation approach

A Computational Fluid Dynamics (CFD) investigation of the impinging lobed jet issuing from a cruciform orifice nozzle described above was conducted in order to test several turbulence models to see which one deals best with the prediction of the wall shear rate for the impinging cross-shaped jet at moderate Reynolds number. Three linear eddy viscosity based turbulence models were tested - SST k-ω, k-ε RNG and realizable k-ε, a second order closure model- RSM and a transitional model - trans SST [7] (a four equations model based on SST k-ω). The main difference between models is the way that Reynolds stresses are taken into account. In the case of eddy viscosity models, Reynolds stresses are modeled and for the second order closer models they are solved.

The computed domain is presented in Fig. 2 as well as the considered boundary conditions for the inlet and for the outlet. The other surfaces were considered as wall. The volume of fluid is composed from two parts separated by a 0.5mm thick plate. The impinging plate is positioned at a distance of $2D_e$ from the exit of the cross shaped orifice.

In the model we considered the same fluid as for the electro-diffusion measurements, which was an aqueous solution of 20 mol/m^3 equimolar potassium ferri/ferrocyanide with 1.5% mass K_2SO_4 as supporting electrolyte. The solution density was 1007 kg/m^3 and its kinematic viscosity 1.065E-06 m^2/s.

The numerical study was performed in ANSYS - Fluent. On the velocity inlet we imposed a 0.1952 m/s uniform velocity corresponding to a flow rate of 3.45E-05 m^3/s (2 l/min). The Reynolds number at the exit of the cross-shaped orifice based on streamwise mean velocity and equivalent diameter of the nozzle was Re = 5290. Simulations are performed in isothermal conditions at constant density, therefore the influence of gravitation can be neglected.

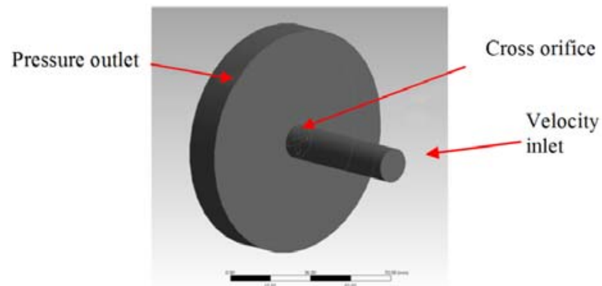

Fig. 2 Computed domain and boundary conditions

The inlet turbulence intensity was imposed as 5.4% being calculated using the empirical relation proposed by Jaramillo [8]: $I = 0.16\,Re^{-1/8}$.

For the pressure-velocity coupling we utilized the SIMPLE algorithm. A second order upwind scheme was used to calculate the convective terms in the equations, integrated with the finite volume method. The convergence criterion imposed for all the variables residuals was 10^{-5}.

A grid dependence study was carried out on several grids: 2.2, 4.6, 5.9 and 9.2 million tetrahedral elements. In all cases, we considered the same boundary conditions. Results obtained by the use of 5.9 and 9.2 million tetrahedral elements are close to the experimental results, this way the final grid was chosen to have 5.9 million elements one. Slices in the interest region through the major and minor planes of the 5.9 million elements mesh are presented in Fig. 3a and Fig. 3b respectively; about 96 hours were needed for each numerical simulation.

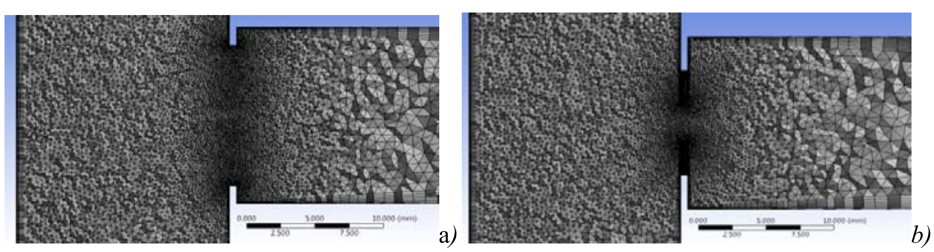

Fig. 3 Detail of the mesh in the interest region a. Major Plane b. minor Plane

For the near-wall modeling, the enhanced wall treatment was used for RSM and k-ε based models as for the k-ω based models, the flow was resolved down to the viscous sublayer. Values of y+ close to 1 are most desirable. Wilcox suggested in [9] to enforce the analytical solution in all points in the computational grid for which $y+ < 2.5$. The results also show that, in general, the error is the largest when the first cell center is located in the region $5 < y+ < 11$, despite the use of correct boundary conditions. In our case, y+ maximum value in the investigated domain was 2.59 considered to be satisfactory, from our experience [10-12].

4. Results and discussions

The wall-shear rate γ reached a maximum value around 14000 s^{-1} measured by the electro-diffusion measurement technique. The comparison between the experimental and the CFD results of the wall-shear rate on the impinging plate are presented in Fig. 4. We compared the wall-shear rate in both Major plane (MP) and minor plane (mP) (Fig. 1 c) as a function of the radial distance from the stagnation point (r = 0).

The best results of this comparison of experimental and numerical simulation values of wall-shear rate were obtained in the Major Plane by the Trans SST turbulence model (Fig. 4 a). On the minor Plane the best results were obtained by another k-ω based turbulence model, k-ω SST (Fig. 4 b).

Both, k-ε RNG (Fig. 4 c) and realizable k-ε (Fig. 4 d) turbulence models tend to underestimate the wall shear rate, for both Major and minor Planes of the jet. On the other hand, the RSM model (Fig. 4 e) underestimates the wall shear rate on the Major Plane. However, on the minor Plane of the first $1.2D_e$ on the radial distance from stagnation point, the wall shear rate numerical values were found to be the closet to the experimental measurement data, with the maximum value around 14000 s^{-1} being as in the experimental case. After $1.2D_e$, the numerical results for wall shear rate were found to be underestimated.

Another interesting aspect was the presence of one inflexion point for the wall shear rate found at $X = 1.4D_e$ on minor plane in the experimental results obtained by electro-diffusion measurement technique. SST k-ω was the only model that has managed to accurately capture the inflection point. Overall, SST k-ω was the turbulence model who gave the best results on predicting the wall shear rate.

Streamwise velocity contours are presented in Fig. 5 on the Major Plane (MP) and on the minor Plane (mP) for PIV experimental results and for all the turbulence models tested within the numerical analysis. In this case, the Trans SST model gave the best results on Major Plane and both k-ω based turbulence models shows good agreement with PIV results for the minor Plane. Overall, Trans SST gave the best results when studying the global dynamics of the flow field in its free jet region. To well predict the radial wall jet region (Fig. 1 a) and the corresponding wall shear stress, the SST k-ω is recommended.

5. Conclusions

RANS modeling of a lobed impinging jet has been tested by means of direct comparison with the experimental data gathered by two different techniques: PIV and electro-diffusion measurements.

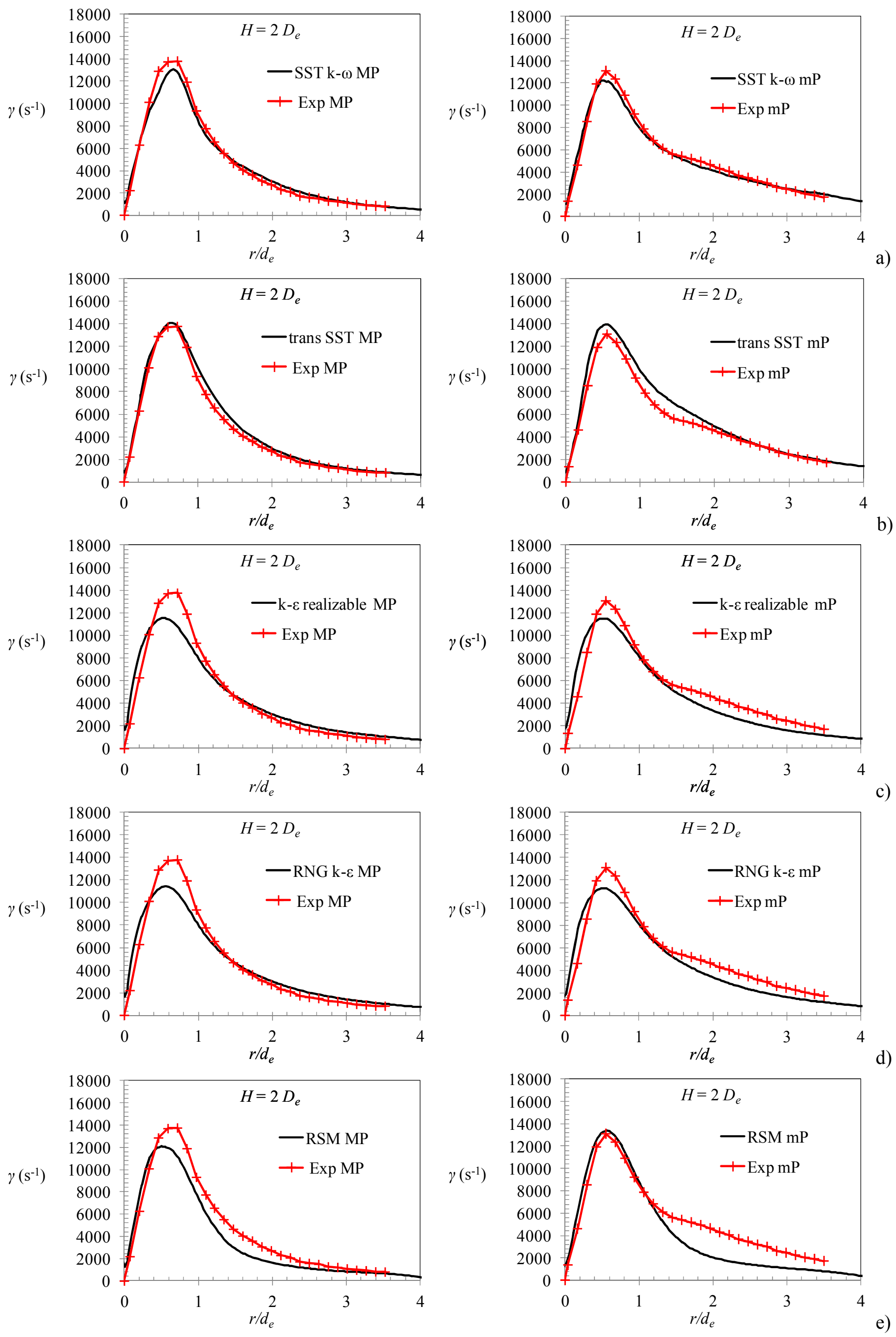

Fig. 4 Comparison between experimental and CFD results on wall-shear rate on impinging plate in Major Plane - MP (left) and minor Plane - mP (right) as a radial distance from stagnation point

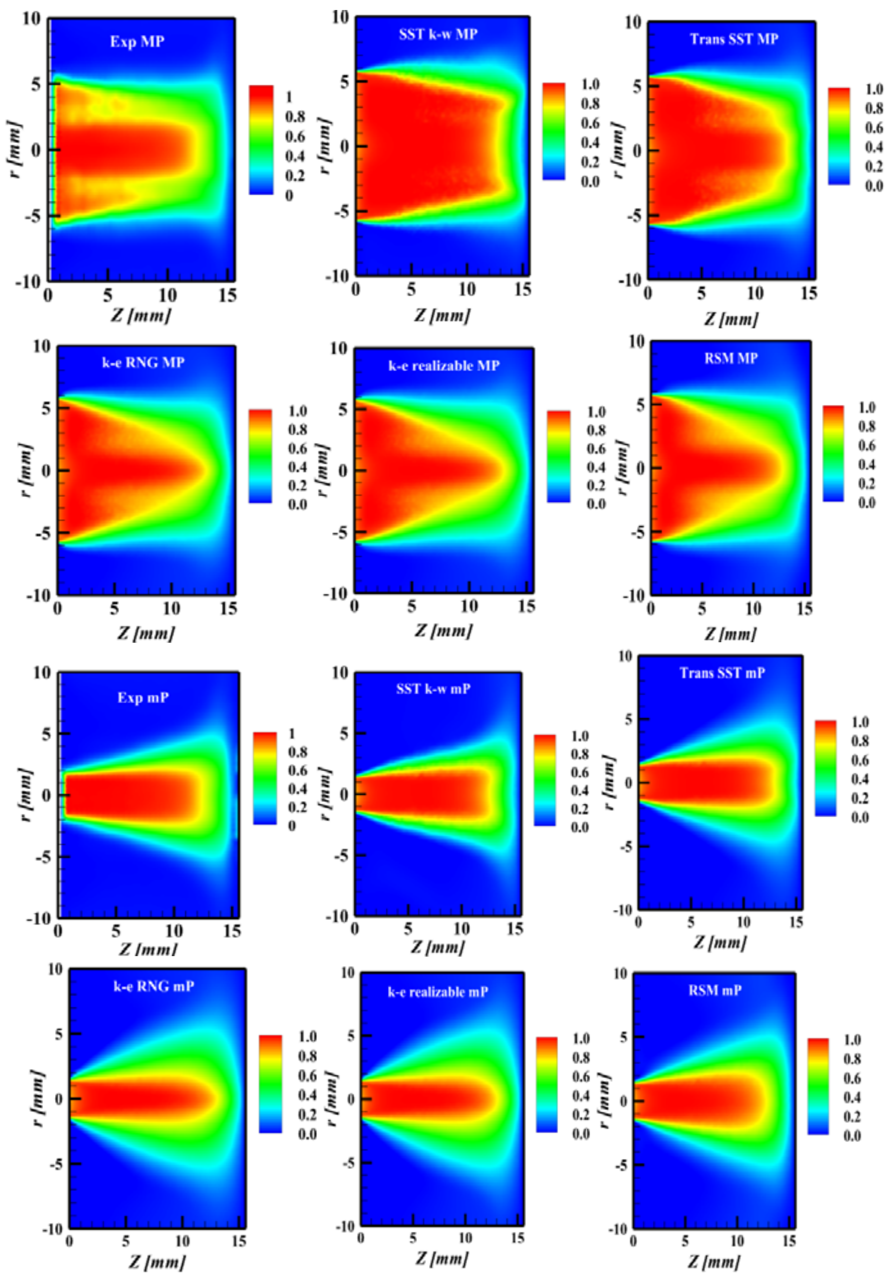

Fig. 5 Streamwise velocity contours on Major Plane (MP) and minor Plane (mP) for PIV experimental results and for all the turbulence models numerical results

The study reveals that none of the five turbulence models tested is able to predict well all impinging jet characteristics in the same time. For example, Trans SST gave the best results in the free jet region and underestimated the shear rate in the minor plane, whereas the k-ω SST which gives the best accuracy in wall shear rate prediction in the two observed planes, is not as satisfactory in the prediction of the free jet region.

Acknowledgment

„This work was supported by the grants of the Romanian National Authority for Scientific Research, CNCS – UEFISCDI, project numbers: PN-II-PD-PCE-2011-3-0099 and PN-II-ID-PCE-2011-3-0835".

R E F E R E N C E S

[1]. Kristiawan, M., et al., *Wall shear rates and mass transfer in impinging jets: Comparison of circular convergent and cross-shaped orifice nozzles.* International Journal of Heat and Mass Transfer, 2012. **55**(1–3): p. 282-293.

[2]. Narayanan, V., J. Seyed-Yagoobi, and R.H. Page, *An experimental study of fluid mechanics and heat transfer in an impinging slot jet flow.* International Journal of Heat and Mass Transfer, 2004. **47**: p. 1827–1845.

[3]. Baydar, E. and Y. Ozmen, *An experimental and numerical investigation on a confined impinging air jet at high Reynolds numbers.* Applied Thermal Engineering, 2005. **25**: p. 409–421.

[4]. Marr, D.R., I.M. Spitzer, and M.N. Glause, *Anisotropy in the breathing zone of a thermal manikin.* Experiments in Fluids, 2008. **44**(4): p. 661-673.

[5]. Meslem, A., et al., *Flow dynamics and mass transfer in impinging circular jet at low Reynolds number. Comparison of convergent and orifice nozzles.* International Journal of Heat and Mass Transfer, 2013. **67**: p. 25-45.

[6]. Phares, D.J., G.T. Smedley, and R.C. Flagan, *The wall shear stress produced by the normal impingement of a jet on a flat surface.* Journal of Fluid Mechanics, 2000. **418**: p. 351-375.

[7]. Ansys, *Fluent 14 user manual.*

[8]. Jaramillo, J.E., et al., *Numerical study of plane and round impinging jets using RANS models.* Numer. Heat Transfer Part B 2008. **54**: p. 213-237.

[9]. Wilcox, D.C., *Turbulence modelling for CFD.* La Canada- California: DCW Industries Inc. 536., 1993.

[10]. Meslem, A., et al., *Numerical study a turbulent jet flow issued from a lobed orifice.* Scientific Journal of Technical University of Civil Engineering in Bucharest - Series: Mathematical Modelling in Civil Engineering, 2010. **6**(3): p. 42-51.

[11]. Croitoru, C., I. Nastase, and F. Bode, *The Influence of the Geometric Form of the Virtual Thermal Manikin on Convective Flow.* Mathematical Modelling, 2011. **7**(4).

[12]. Meslem, A., et al., *Optimization of a Lobed Perforated Panel Diffuser - A Numerical Study of Orifice Arrangement.* International Journal of Ventilation, 2012. **11**(3): p. 255-270.